ACCOUNTS
of chemical research

Proton-Mediated Chemistry and Catalysis in a Self-Assembled Supramolecular Host

MICHAEL D. PLUTH, ROBERT G. BERGMAN,* AND
KENNETH N. RAYMOND*

Department of Chemistry, University of California, Berkeley, and Division of Chemical Sciences, Lawrence Berkeley National Laboratory, Berkeley, California, 94720-1460

RECEIVED ON APRIL 10, 2009

CONSPECTUS

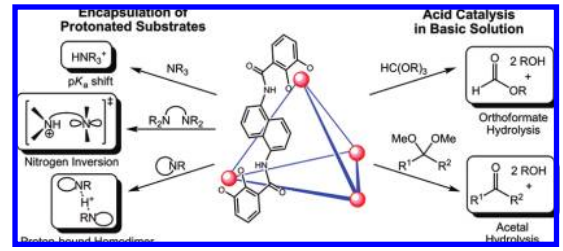

Synthetic supramolecular host assemblies can impart unique reactivity to encapsulated guest molecules. Synthetic host molecules have been developed to carry out complex reactions within their cavities, despite the fact that they lack the type of specifically tailored functional groups normally located in the analogous active sites of enzymes. Over the past decade, the Raymond group has developed a series of self-assembled supramolecules and the Bergman group has developed and studied a number of catalytic transformations. In this Account, we detail recent collaborative work between these two groups, focusing on chemical catalysis stemming from the encapsulation of protonated guests and expanding to acid catalysis in basic solution.

We initially investigated the ability of a water-soluble, self-assembled supramolecular host molecule to encapsulate protonated guests in its hydrophobic core. Our study of encapsulated protonated amines revealed rich host−guest chemistry. We established that self-exchange (that is, in−out guest movement) rates of protonated amines were dependent on the steric bulk of the amine rather than its basicity. The host molecule has purely rotational tetrahedral (*T*) symmetry, so guests with geminal *N*-methyl groups (and their attendant mirror plane) were effectively desymmetrized; this allowed for the observation and quantification of the barriers for nitrogen inversion followed by bond rotation. Furthermore, small nitrogen heterocycles, such as *N*-alkylaziridines, *N*-alkylazetidines, and *N*-alkylpyrrolidines, were found to be encapsulated as proton-bound homodimers or homotrimers. We further investigated the thermodynamic stabilization of protonated amines, showing that encapsulation makes the amines more basic in the cavity. Encapsulation raises the effective basicity of protonated amines by up to 4.5 pK_a units, a difference almost as large as that between the moderate and strong bases carbonate and hydroxide.

The thermodynamic stabilization of protonated guests was translated into chemical catalysis by taking advantage of the potential for accelerating reactions that take place via positively charged transition states, which could be potentially stabilized by encapsulation. Orthoformates, generally stable in neutral or basic solution, were found to be suitable substrates for catalytic hydrolysis by the assembly. Orthoformates small enough to undergo encapsulation were readily hydrolyzed by the assembly in basic solution, with rate acceleration factors up to 3900 compared with those of the corresponding uncatalyzed reactions. Furthering the analogy to enzymes that obey Michaelis−Menten kinetics, we observed competitive inhibition with the inhibitor NPr_4^+, thereby confirming that the interior cavity of the assembly was the active site for catalysis. Mechanistic studies revealed that the assembly is required for catalysis and that the rate-limiting step of the reaction involves proton transfer from hydronium to the encapsulated substrate. Encapsulation in the assembly changes the orthoformate hydrolysis from an A-1 mechanism (in which decomposition of the protonated substrate is the rate-limiting step) to an A-S_E2 mechanism (in which proton transfer is the rate-limiting step). The study of hydrolysis in the assembly was next extended to acetals, which were also catalytically hydrolyzed by the assembly in basic solution. Acetal hydrolysis changed from the A-1 mechanism in solution to an A-2 mechanism inside the assembly, where attack of water on the protonated substrate is rate limiting.

This work provides rare examples of assembly-catalyzed reactions that proceed with substantial rate accelerations despite the absence of functional groups in the cavity and with mechanisms fully elucidated by quantitative kinetic studies.

Published on the Web 07/10/2009 www.pubs.acs.org/acr
10.1021/ar900118t CCC: $71.50

Introduction

The process of spontaneous self-assembly has gained importance in many disciplines of chemistry. By exploitation of the thermodynamically driven assembly of predesigned subunits, the additivity of the otherwise weak, frequently noncovalent interactions plays a necessary role in the formation of a final structure that often has properties that are distinct from those of any of the individual subunits.[1,2] The complexity of the final molecular structures obtained through self-assembly has evolved considerably since the pioneering work by Lehn, Cram, Pedersen, and Breslow and now includes supramolecules able to promote both stoichiometric and catalytic reactions.[2−9] The interior cavities, generally protected from bulk solution, provide a unique environment for encapsulated guest molecules and can stabilize otherwise unstable species or lead to enhanced reactivity and selectivity. Supramolecular catalysts can also activate otherwise unreactive substrates without the use of distinct covalent interactions between the catalyst and substrate. Because adjacent fields of catalysis have shown remarkable improvements in scope and selectivity, catalytic supramolecular architectures offer a unique opportunity for the study of how weak interactions work in concert to provide often remarkable results.

In the study of how supramolecular assemblies are able to activate otherwise unreactive molecules through encapsulation, the analogy to enzymatic systems is natural. The remarkable specificity of enzymes and their ability to greatly accelerate chemical reactions in water, at physiological pH and temperature, are feats arguably unattained by any synthetic system. Similarly, the functional group availability and requirements of enzyme active sites maintain a precision that synthetic chemists have yet to duplicate. Although the complexity of the catalysis occurring in enzyme active sites will likely continue to both puzzle and amaze scientists for decades to come, synthetic supramolecular architectures offer the opportunity to study how molecular sequestration can affect the reactivity of encapsulated guests.

The synergistic combination of charge, dielectric, shape, size, and functional group availability defines the guest-binding preferences of synthetic host molecules. The steric constraints of the interior cavities of molecular hosts often attenuate the entropic penalty for reactions requiring preorganization. Similarly, functional group availability, either on the interior or on the periphery of the host cavity, can preorganize substrates in reactive conformations to stabilize reactive intermediates. Alternatively, steric confinement can accelerate bimolecular reactions if binary pairs of the reactants are preferentially encapsulated, effectively increasing the local concentration of the reactants. By the appropriate choice of substrates with complementary interactions with the host molecule, large rate accelerations, changes in selectivity, or shifts in the thermodynamic properties of encapsulated guests have been demonstrated.[10−15] In this Account, we document how the hydrophobic cavity of a self-assembled supramolecular host is able to thermodynamically shift the acid−base equilibrium of encapsulated guests and how we translated this stabilization into chemical catalysis.

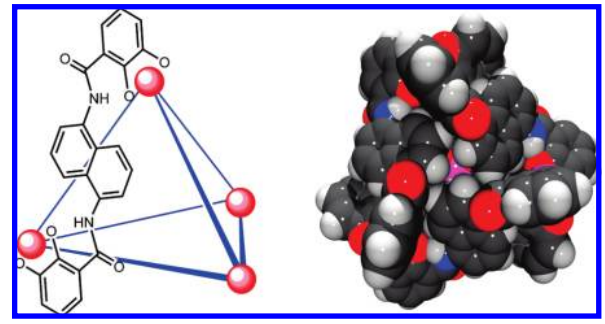

FIGURE 1. Schematic (left) and space-filling model (right) of **1**.

The $[Ga_4L_6]^{12-}$ Host. The strategy of predesigned self-assembly based on incommensurate coordination number has been used by the Raymond group to generate a number of different supramolecular architectures.[16,17] The tetrahedral $[Ga_4L_6]^{12-}$ (**1**) assembly has purely rotational *T* symmetry generated from the four metal atoms and six naphthalene-based ligands defining the vertices and edges of the structure, respectively (Figure 1). The chirality generated from the tris-bidentate coordination of one metal vertex is transferred to the other vertices due to the ligand rigidity, thereby requiring exclusive formation of the homochiral ΔΔΔΔ and ΛΛΛΛ enantiomers. Although other C_2-symmetric ligands generate tetrahedral M_4L_6 assemblies, the naphthalene ligand provides a host molecule with desirable properties. For example, **1** is water-soluble, stays intact during guest exchange, forms without a thermodynamically templating guest, is resolvable into its enantiomers, and provides a hydrophobic interior cavity of up to 450 Å^3.[18−20] We have previously demonstrated the ability of **1** to modify the reactivity of both stoichiometric and catalytic transition metal mediated reactions as well as its ability to act as a catalyst.[21−23]

Protonated Guests

Encapsulation Scope and Exchange Dynamics. The hydrophobic interior of **1** is able to stabilize otherwise water-reactive species such as tropylium, cationic phosphine−acetone adducts, and iminium ions.[24−26] Although these reactive species are normally only observed in either anhydrous organic

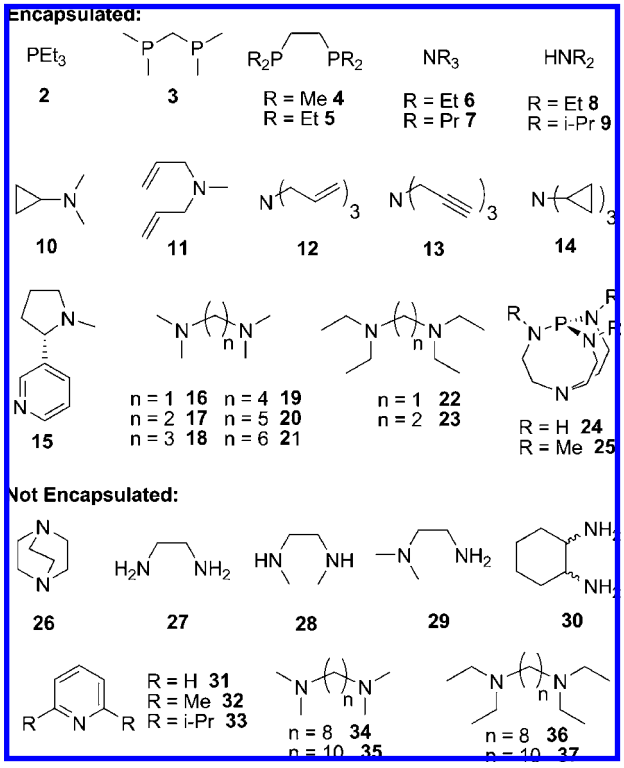

FIGURE 2. Scope of protonated guests investigated in **1**.

or acidic aqueous solution, the host–guest complexes of the species were persistent, and could be studied in either neutral or basic aqueous solution, thus prompting our investigation of protonated guests encapsulated in **1**.

The addition of small amines or phosphines to an aqueous solution of **1** produces new ^{1}H NMR resonances corresponding to 1:1 host–guest complexes.[27] For encapsulated phosphines, monoprotonation was determined by ^{31}P NMR spectroscopy in H_2O and D_2O by analysis of the $^1J_{PH}$ or $^1J_{PD}$ coupling constants. For the encapsulated amines, monoprotonation was confirmed by the pH dependence of encapsulation and the kinetic observation of proton transfer in encapsulated diamines (*vide infra*).[28] For suitably large guests, such as pro-azaphosphatranes (**24**, **25**), mass spectra confirming protonation were obtained.

A variety of potential guests were screened in order to determine the scope of encapsulation of protonated amines in **1** (Figure 2). A number of trends can be extracted from the guest screening. Small tertiary diamines (**16**–**23**) are readily encapsulated, although extension of the methylene backbone to eight or ten methylene units (**34**–**37**) prohibits encapsulation. Both secondary (**8**, **9**) and tertiary monoamines (**10**, **11**) are encapsulated, but primary diamines (**27**, **29**, **30**) are not encapsulated due to the greater solvation in free solution and the large associated enthalpy loss of desolvation required for encapsulation. Substituted pyridines (**31**–**33**) are not encapsulated, likely due to the low basicity of these guests. Nicotine (**15**), however, is encapsulated, although protonation likely occurs at the more basic pyrrolidine nitrogen.

TABLE 1. Self-Exchange Rates and pK_a's for Selected Encapsulated Amines

amine	pK_a	k_{277} (s^{-1})
6	10.7	46(9)
7	10.7	0.31(4)
10	8.5	5.3(3)
12	8.3	5.4(6)
13	8.1	4.4(6)
14	6.4	1.1(1)
15	10.6	1.0(5)
17	9.1	47(9)
18	9.8	1.1(2)
19	9.8	0.24(3)[a]
21	9.8	1.9(3)
23	10.8	0.13(2)[a]

[a] Measured at 320 K.

Our interest in guest exchange dynamics of host–guest systems prompted our investigation of the kinetics of guest exchange, specifically whether the guest exchange rates were determined by the basicity or size of the guest. The self-exchange rates of the encapsulated protonated amines were measured using the selective inversion recovery (SIR) method[29] at 277 K, pD 13.0, 500 mM KCl, 11 mM **1**, and 55 mM amine. A comparison of the exchange rates with the pK_a of the guests (Table 1) shows that the exchange rate is dependent on the size, rather than the basicity, of the guest. This size dependence is exemplified by comparing **6** and **7**, which have identical basicities but very different exchange rates. The activation parameters determined for guest self-exchange for **19** and **23** were similar to those determined for NR_4^+ guests, suggesting that the same guest exchange mechanism was operative.

Nitrogen Inversion Bond Rotation (NIR). In screening protonated diamines, we observed that in some cases the geminal *N*-methyl groups appeared as two NMR resonances whereas in other cases only one resonance was observed. Since the purely rotational *T* symmetry of **1** provides only C_2 and C_3 rotational symmetry to encapsulated guests and subsequently removes any mirror symmetry normally observed, we surmised that the difference in the number of NMR resonances was due to interchange of the *N*-methyl groups on the NMR time scale through the process of nitrogen inversion followed by bond rotation (NIR) (Figure 3).[28] Cleavage of the N–H hydrogen bond (a) allows one nitrogen stereocenter to invert (b), rotate (c), and finally reform the hydrogen bond (d), leading to a net interchange of the geminal *N*-methyl groups. Variable-temperature ^{1}H NMR experiments on the encapsulated monoprotonated diamines showed coalescence behavior consistent with this mechanism (Figure 3).

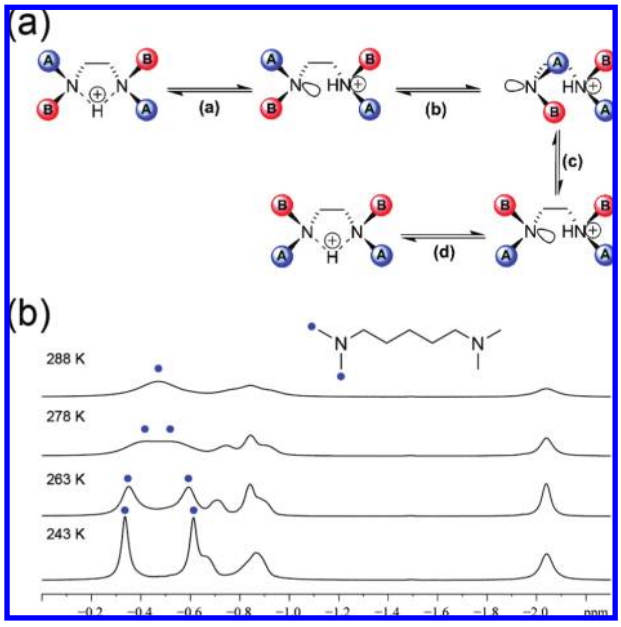

FIGURE 3. Schematic (top) for the NIR process resulting in the interchange of the geminal *N*-methyl groups and variable temperature ^{1}H NMR (bottom) showing coalescence of the geminal *N*-methyl groups.[28]

In order to confirm that the observed coalescence behavior was due to the NIR process rather than guest ejection followed by NIR in free solution and subsequent reencapsulation, the activation parameters for guest exchange were measured using Eyring analysis. If the free energy of activation for guest exchange ($\Delta G^{\ddagger}_{exch}$), calculated at the coalescence temperature, is greater than the free energy of activation measured for the coalescence process ($\Delta G^{\ddagger}_{coal}$), then NIR is occurring inside **1** ($\Delta\Delta G^{\ddagger} > 0$). Alternatively, if $\Delta G^{\ddagger}_{exch} < \Delta G^{\ddagger}_{coal}$, then it is possible that the amine is ejected from **1**, undergoes NIR outside of the assembly, and is then reencapsulated ($\Delta\Delta G^{\ddagger} \leq 0$). For each of the diamines investigated, $\Delta\Delta G^{\ddagger} > 0$ thereby confirming that the NIR process is occurring inside **1** (Figure 4). For each of the monoamines investigated, $\Delta\Delta G^{\ddagger}$ is statistically zero, which suggests that the amine is ejected from **1** and undergoes NIR in solution and is then reencapsulated.

Encapsulation of Proton-Bound Multimers. Based on the observation that the diamines were able to intramolecularly chelate one proton, we hypothesized that two separate amines could be encapsulated in **1** by coordinating a single proton. Cyclic amines were chosen based on their reduced degrees of rotational freedom, which should attenuate the entropic penalty for the simultaneous encapsulation of multiple guests (Figure 5).[30]

Screening the cyclic amines with **1** showed proton-bound homodimer for *N*-methyl, isopropyl, and *tert*-butyl aziridine (**43**, **45**, **46**); *N*-isopropyl and *tert*-butyl azetidine (**48**, **49**); and

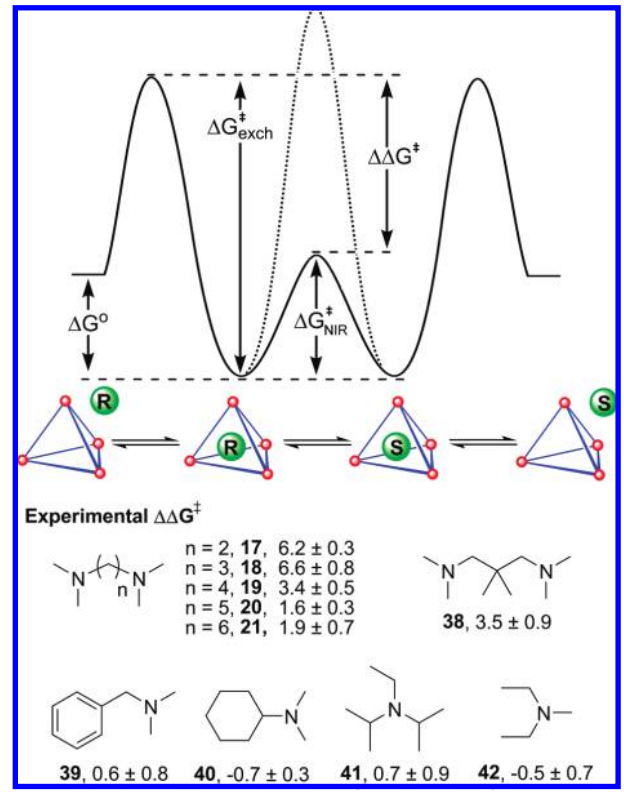

FIGURE 4. Energy diagram (top) for amine exchange and inversion in **1**. Solid line corresponds to $\Delta G^{\ddagger}_{NIR} < \Delta G^{\ddagger}_{exch}$; dotted line corresponds to $\Delta G^{\ddagger}_{exch} < \Delta G^{\ddagger}_{NIR}$. Bottom panel gives $\Delta\Delta G^{\ddagger}$ values (kcal/mol) of the investigated amines.[28]

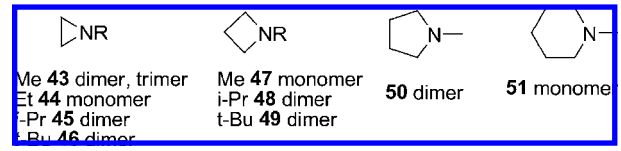

FIGURE 5. Scope of cyclic amines encapsulated in **1**.

N-methyl pyrrolidine (**50**). As the concentration of **43** was increased, exclusive homotrimer encapsulation was observed. Proton-bound heterodimer formation was investigated by screening binary mixtures of the cyclic amines (**43**−**50**) with **1**. Only for the binary mixture of **45** and **50** was exclusive proton-bound heterodimer observed.

Thermodynamic Stabilization of Protonated Amines. With a greater understanding of the scope of amine encapsulation in **1**, the thermodynamics of guest encapsulation were explored. The observation that protonated amines were encapsulated in **1** even when the pH of the solution was above the pK_a of the protonated amine suggested a strong intracavity stabilization. Shifts in the basicity of encapsulated compound have been observed of up to 4 pK_a units in cucurbiturils and functionalized cyclodextrins and have been estimated to be 5−7 pK_a units upon encapsulation into the interior of carbosilane nanocages.[31−35] The thermodynamic

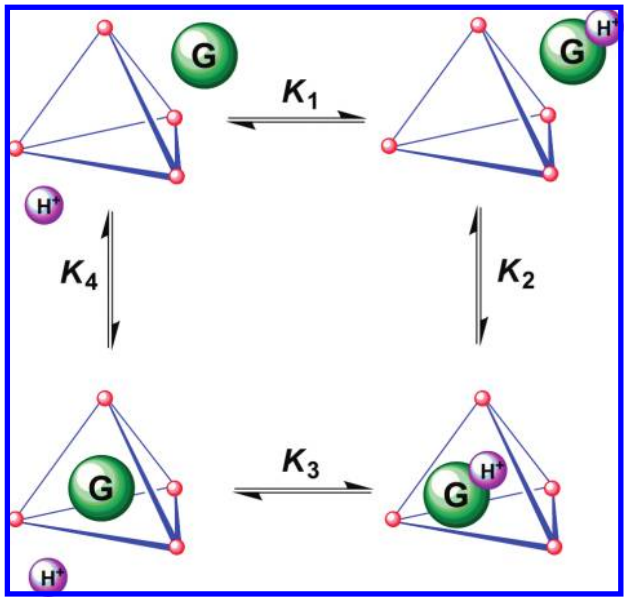

FIGURE 6. Thermodynamic cycle for the encapsulation of protonated guests in **1**.

cycle for the encapsulation of protonated amines is shown in Figure 6. K_1 defines the acid−base equilibrium of the amine in free solution and K_2 defines the binding constant of the protonated amine in **1**. Although we did not observe neutral amines encapsulated in **1**, we have previously shown that neutral guests can enter **1**[36−38] and K_4 defines the neutral guest encapsulation equilibrium. The thermodynamic cycle can be completed by K_3, which is the acid−base equilibrium for the encapsulated amine corresponding to the effective basicity of the encapsulated amine in **1** (pK_{eff}).

In order to determine the magnitude of the thermodynamic stabilization, the extent of amine encapsulation was monitored in equimolar solutions of **1** and amine as a function of pH. From the equilibrium measurements and the pK_a of the amines, the binding affinities of the protonated guests were determined. In all cases, encapsulation in **1** greatly favored formation of the protonated substrate, effectively making the amines more basic upon encapsulation (Table 2).[27] Although this stabilization is often referred to as a pK_a shift, in the present case it is more accurately referred to as a shift in effective basicity because neither the neutral amines nor water/hydroxide were directly observed inside of **1**.

Acid Catalysis in Basic Solution

Orthoformate Hydrolysis. Based on the large thermodynamic stabilization of protonated amines in **1**, we wanted to use the stabilization for chemical catalysis. If a protonated transition state of a reaction could be thermodynamically stabilized analogously to the encapsulated protonated amines,

TABLE 2. Thermodynamic Parameters for Encapsulation of Protonated Guests in **1**

amine	pK_a	$\log(K_{eff})$	$-\Delta G°$ (kcal/mol)	effective basicity (pK_{eff})
6	10.7	2.1	2.9	12.8
7	10.7	2.7	3.7	13.4
9	10.8	3.4	4.6	14.2
10	8.5	3.3	4.5	11.8
12	8.3	4.4	6.0	12.7
13	8.1	4.5	6.1	12.6
14	6.4	3.2	4.4	9.6
15	10.6	2.8	3.8	13.4
17	9.1	3.1	4.2	12.2
18	9.8	3.8	5.2	13.6
19	9.8	3.8	5.2	13.6
21	9.8	4.1	5.6	13.9
23	10.8	3.5	4.8	14.3

SCHEME 1

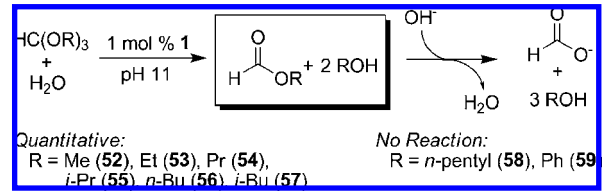

then **1** should act as a catalyst for acid-catalyzed reactions. In order to abate the problem of product inhibition, the product should either be a poor guest or undergo further reaction in solution to prohibit reencapsulation. Based on these criteria, orthoformates, which are stable in neutral or basic solution but undergo acid-catalyzed hydrolysis in acid, were the first hydrolysis substrates tested in **1**.[39,40] In basic solution, the formate ester product would be quickly hydrolyzed to produce formate anion, which could not bind to **1** due to Coulombic repulsion.

In order to test the viability of **1** to act as a catalyst for orthoformate hydrolysis, triethyl orthoformate (**53**) was added to **1** in basic solution.[41,42] Monitoring the reaction by ^{1}H NMR revealed the production of both ethanol and formate anion. In the absence of **1**, no hydrolysis of **53** was observed over the same time period. Addition of NEt_4^+, a strongly binding guest, inhibited the catalysis and confirmed the catalytic importance of **1**. Other small alkyl orthoformates (**52**−**57**) were also readily hydrolyzed by **1** at pH 11, 50 °C, whereas larger substrates, such as tripentyl (**58**) or triphenyl orthoformate (**59**), were too large to enter **1** and remained unreacted (Scheme 1).

The mechanism of orthoformate hydrolysis in **1** was investigated in order to further understand how **1** participates in the hydrolysis of this class of compounds. While keeping the pH and concentration of **1** constant, the substrate concentration was varied to reveal Michaelis−Menten saturation kinetics. At

saturation, the hydrolysis of **53** was pseudo-zeroth order as expected. Working under saturation conditions, the reaction was determined to be first-order in both H^+ concentration and **1** concentration leading to the rate law rate = $k[H^+][\mathbf{1}][\text{substrate}]$, which at saturation reduces to rate = $k'[H^+][\mathbf{1}]$.

Under standard catalytic conditions, upfield ^1H NMR resonances corresponding to host−substrate complex were not observed, but rather the unencapsulated substrate resonances were broadened. Addition of NEt_4^+ to the reaction sharpened the substrate resonances to the line width normally observed in solution, thereby suggesting fast orthoformate guest exchange. Investigation of the stoichiometric reaction at a near saturated solution of **1** revealed a kinetically stable host−guest complex. In order to confirm that the resting state of the reaction was the encapsulated neutral orthoformate, $H^{13}C(OEt)_3$ (^{13}C-**53**) was investigated with **1**. Under stoichiometric conditions, the ^{13}C resonance of ^{13}C-**53** was shifted upfield by 2.5 ppm, which is consistent with encapsulation in **1**, and the $^1J_{CH}$ coupling constant remained unchanged compared with that of free ^{13}C-**53**, thus confirming that the neutral orthoformate, rather than possible protonated orthoformate or hemiorthocarboxylate intermediate, was the resting state. Since our initial kinetic observation of neutral guest encapsulation, we have subsequently expanded the chemistry of encapsulated neutral guests to include linear and cyclic alkanes, simultaneous encapsulation of multiple aromatic guests, and use of **1** to lower the rotational barrier for encapsulated tertiary amides.[36−38]

In order to obtain more information about the rate-determining step of the reaction, the activation parameters and solvent isotope effect (SIE), $k(H_2O)/k(D_2O)$, of the k_{cat} Michaelis rate constant were determined. These kinetic parameters provide information about the role of protonation in the rate-limiting step and the mechanism of decomposition of the activated transition-state complex. Eyring analysis of k_{cat} at different temperatures afforded $\Delta G^{\ddagger}_{298K} = 22(2)$ kcal/mol, $\Delta H^{\ddagger} = 21(1)$ kcal/mol, and $\Delta S^{\ddagger} = -5(1)$ eu, and measurement of the k_{cat} rate constant in H_2O and D_2O revealed a normal SIE of 1.6. These parameters strongly support an A-S_E2 mechanism in which proton transfer between protonated water and the substrate is rate-limiting.[39,40] This is in contrast to the A-1 mechanism for hydrolysis of **53** in free solution in which protonation of the substrate is fast and decomposition of the protonated substrate is the rate-limiting step (Figure 7).[39,40]

The overall mechanism for orthoformate hydrolysis in **1** is outlined in Figure 8. Initially, the neutral orthoformate is encapsulated in **1** in a fast pre-equilibrium to generate the resting state. The subsequent rate-limiting step involves proton transfer from protonated water to the substrate. The observed SIE and activation parameters suggest that at least the first hydrolysis step following the rate-limiting protonation occurs inside of **1** after which any of the resultant species can undergo either acid- or base-catalyzed decomposition.

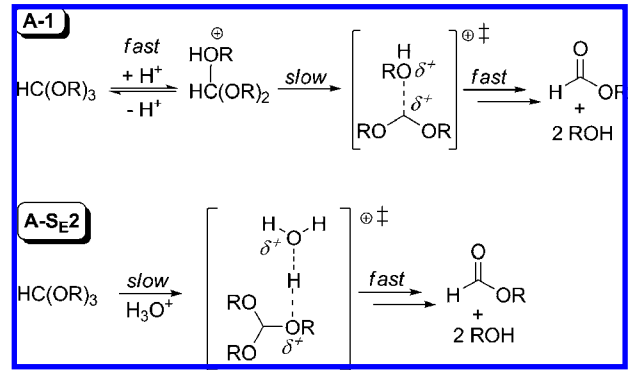

FIGURE 7. Comparison of A-1 and A-S_E2 mechanisms for orthoformate hydrolysis. Hydrolysis of **53** proceeds through an A-1 mechanism in free solution but an A-S_E2 mechanism in **1**.

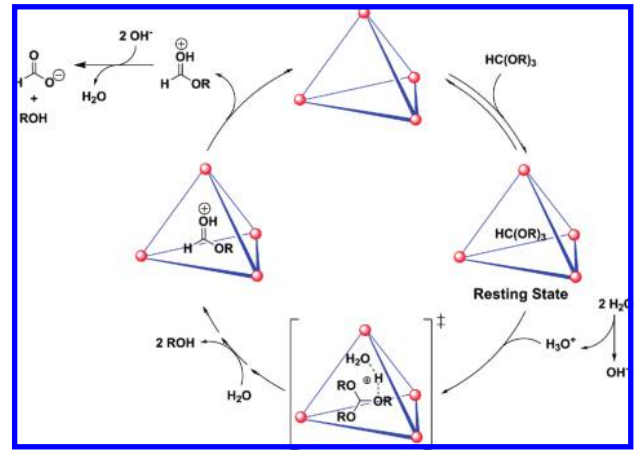

FIGURE 8. Proposed mechanism for catalytic hydrolysis of orthoformates in **1**.[42]

To further the analogy to enzymatic catalysts that exhibit Michaelis−Menten kinetics, we sought to demonstrate that suitable guests can competitively inhibit the catalysis in **1**. In order for competitive inhibition to occur, the inhibitor must reversibly bind to the same site that is responsible for catalysis. At a suitably high concentration of substrate, the substrate will completely displace the inhibitor, leading to a restoration of the catalytic activity. In order to test for competitive inhibition, the hydrolysis rates of **53** were measured in the presence of varying amounts of the strongly binding guest NPr_4^+. The resultant saturation curves were compared using an Eadie−Hofstee plot (Figure 9).[43,44] The observed intersection on the *y*-axis signified that at infinite substrate concentration the maximum reaction velocity is independent of the amount of inhibitor and confirmed competitive inhibition.

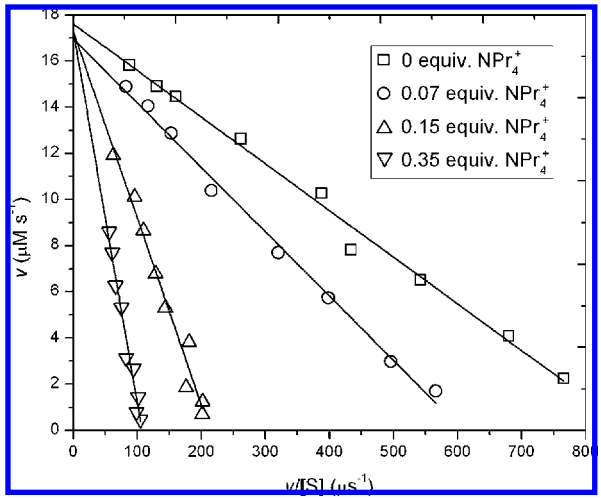

FIGURE 9. Eadie−Hofstee plot showing competitive inhibition by NPr_4^+ for the hydrolysis of **53** in **1**.[41]

In order to compare the rate acceleration of orthoformate hydrolysis in **1** to the uncatalyzed reaction, the k_{cat} rate constants determined from the Michaelis−Menten analysis were compared with those of the background reaction and revealed large rate accelerations of up to 3900 for **54**. Based on the fast pre-equilibrium with respect to the k_{cat} step, the Michaelis constant, K_M, can be viewed as a dissociation constant for the encapsulated substrate. As the hydrophobicity of the substrates increases, a concomitant increase in binding affinity is observed with the two propyl isomers, **54** and **55**, having the highest affinities for **1**. Although **54** and **55** are similarly sized, encapsulation of the *n*-propyl substrate results in a greater loss of conformational freedom, which helps to explain the difference in rate accelerations. Comparing the specificity factor, k_{cat}/K_M, provides a measure of how efficiently different substrates compete for the active site of **1**. The specificity factor increases with substrate size up to a maximum for **54** suggesting an ideal balance of hydrophobicity and shape for encapsulation of this molecule, which is consistent with the large observed rate acceleration. The catalytic proficiency, $(k_{cat}/K_M)/k_{uncat}$, is a measure of how encapsulation affects the transition state stabilization with respect to the uncatalyzed reaction. For the smaller substrates **52**−**54**, as the alkyl change length increases, the catalytic proficiency also increases, thereby suggesting better transition state recognition (Table 3). Although **54** and **55** have similar catalytic proficiencies, **54** maintains a larger rate acceleration that can be rationalized by the ground-state stabilization of **55**. The kinetic analysis of the catalysis in **1** is consistent with the idea that both transition-state and ground-state effects play important roles in the catalysis.

TABLE 3. Tabulation of Kinetic Parameters for Orthoformate Hydrolysis in **1**

substrate	k_{cat} (s^{-1})	K_M (mM)	k_{cat}/K_M (M^{-1} s^{-1})	$(k_{cat}/K_M)/k_{uncat}$ (M^{-1})	k_{cat}/k_{uncat}
52	5.7×10^{-3}	24.0	0.238	6.4×10^3	150
53	8.1×10^{-3}	21.5	0.275	1.9×10^4	560
54	1.8×10^{-2}	19.6	0.918	2.0×10^5	3900
55	3.9×10^{-3}	7.69	0.502	1.2×10^5	890

SCHEME 2

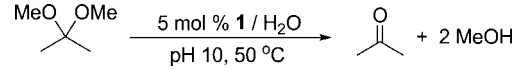

Acetal Hydrolysis. Prompted by the ability of **1** to catalyze orthoformate hydrolysis, we expanded our study to the acid-catalyzed hydrolysis of acetals.[45,46] The stability of acetals in neutral or basic solution makes them a common protecting group for aldehydes and ketones in organic synthesis. Common methods for hydrolyzing acetals almost always employ the use of either Brønsted acid or Lewis acid catalysts with only a few examples of hydrolysis in neutral or slightly basic solution.[47,48]

The mediation of acid-catalyzed acetal hydrolysis by **1** was first investigated using 2,2-dimethoxypropane (**60**) as a substrate. Addition of **60** to a solution of **1** in H_2O at pH 10 quickly produced the expected hydrolysis products (Scheme 2). The catalytic reaction could be inhibited by addition of NEt_4^+, again confirming the importance of **1** in the reaction.

The substrate scope of acetal hydrolysis in **1** was probed at pH 10 in H_2O at 50 °C using 5 mol % **1** with respect to the substrate (Figure 10). Smaller substrates (**60**−**72**) able to fit into the cavity of **1** are readily hydrolyzed, while larger substrates (**73**, **74**) remain unreacted. Under the reaction conditions, excellent NMR conversion was observed in all cases and suitable bulky ketone products could be isolated in good yields (79−92%).

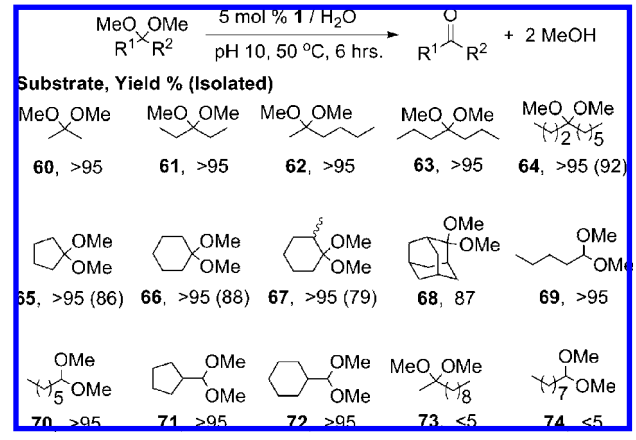

FIGURE 10. Scope of acetal hydrolysis in **1**.

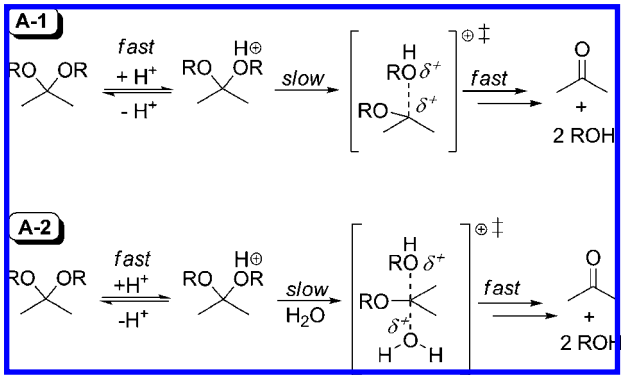

FIGURE 11. Comparison of A-1 and A-2 mechanisms for acetal hydrolysis. Hydrolysis of **60** proceeds through an A-1 mechanism in free solution but an A-2 mechanism in **1**.

Mechanistic studies were undertaken using **60** as the substrate in order to understand the mechanism of acetal hydrolysis in **1** and for comparison to the mechanism determined for orthoformate hydrolysis. At constant pH and concentration of **1**, the substrate concentration was varied to reveal Michaelis–Menten saturation kinetics. At saturation, hydrolysis of **60** is pseudo-zeroth-order and the reaction was determined to be first-order in both H^+ concentration and **1** concentration, providing the final rate law rate = $k[H^+]$-[**1**][substrate], which at saturation reduces to rate = $k'[H^+][\mathbf{1}]$.

Under the standard catalytic conditions for **60**, the substrate ^{1}H NMR resonances were broadened but upfield resonances corresponding to encapsulated substrate were not observed. Addition of NEt_4^+ sharpened the substrate resonances, which suggested that the broadening was due to fast guest exchange. For larger substrates such as **68**, a 1:1 host–guest complex was observed by ^{1}H NMR, indicating slow substrate exchange on the NMR time scale. During the hydrolysis reaction of **68**, new resonances corresponding to the encapsulated product 2-adamantanone (**75**) were observed. By independently measuring the total amount of neutral guest in solution, both free and encapsulated, as a function of [**1**], the effective binding constants were measured as 3400 M^{-1} (**68**) and 700 M^{-1} (**75**).

To further investigate the rate-limiting step of the reaction, the activation parameters and the SIE were determined for the k_{cat} step. Eyring analysis of k_{cat} revealed activation parameters of $\Delta G^{\ddagger}_{298K}$ = 23(1) kcal/mol, $\Delta H^{\ddagger}$ = 21(1) kcal/mol, and $\Delta S^{\ddagger}$ = −9(1) cal/(mol K), and measurement of k_{cat} in H_2O and D_2O afforded an inverse SIE of 0.62. Both of these parameters support an A-2 hydrolysis mechanism in which a fast protonation pre-equilibrium exists followed by the rate-limiting attack of water on the protonated substrate (Figure 11). Hydrolysis of **60** in free solution proceeds through an A-1 mechanism in which unimolecular decomposition of the protonated substrate is the rate-limiting step, characterized by a positive entropy of activation and an inverse SIE.[39,40] As was observed for orthoformates, the mechanism of hydrolysis is changed in **1**.

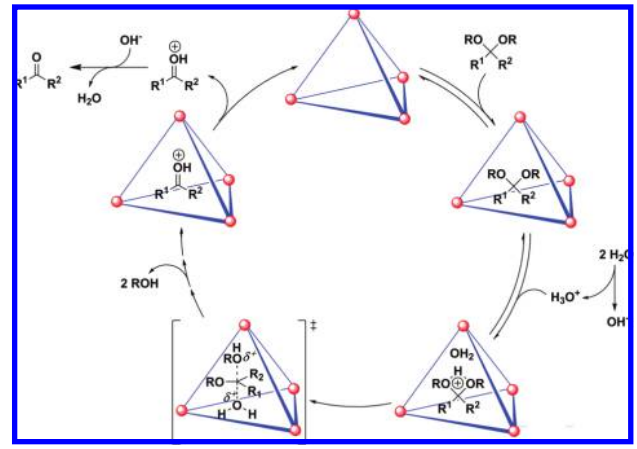

FIGURE 12. Proposed mechanism for acetal hydrolysis in **1**.[46]

The full catalytic cycle for acetal hydrolysis in **1** is shown in Figure 12. Encapsulation of the neutral acetal substrate generates the catalyst resting state. Subsequent protonation of the encapsulated substrate by H_3O^+ leads to the rate-limiting attack of water on the protonated substrate. After this initial rate-limiting hydrolysis step, any of the remaining steps of the reaction can be either acid or base catalyzed so it is not possible to determine whether the entire hydrolysis occurs inside of **1** or the substrate is ejected into bulk solution after the rate-limiting step.

In order to compare the rate acceleration of the catalyzed over the uncatalyzed reaction, the k_{cat} rate constants from Michaelis–Menten studies were compared with those of the background hydrolysis reaction. This analysis revealed sizable accelerations (k_{cat}/k_{uncat}) of 190 for **60** and 980 for 1,1-dethoxyethane (**76**). Comparison of the K_M revealed that the more water-soluble **76** maintains a lower affinity for the interior of **1** than does **60** (**60**, 8.09 mM; **76**, 31.1 mM). Comparison of the specificity factor, k_{cat}/K_M, for **60** and **76** revealed values of 0.099 and 0.153 M^{-1} s^{-1}, respectively, thereby showing that **76** is more readily hydrolyzed than **60** by the assembly. The catalytic proficiency ($(k_{cat}/K_M)/k_{uncat}$) for the two substrates **60** and **76** was quite similar (**60**, 2.28 × 10^4 M^{-1}; **76**, 3.12 × 10^4 M^{-1}), suggesting that the difference in ground state binding (K_M) is primarily responsible for the difference in the rate acceleration.

Conclusions and Future Directions

Until relatively recently, the field of molecular recognition (host–guest chemistry) was dominated by binding studies. More recently, attention has begun to focus on the challenge of carrying out stoichiometric and even catalytic chemical

reactions inside host cavities, with the goal of utilizing synthetic systems to help understand the factors that control catalysis by enzymes and other complex catalysts in which the critical transformations take place in one or more localized active sites. The chemistry reviewed in this Account highlights the selectivity of a supramolecular host molecule in guest binding and the ability of the host to modulate the chemistry of encapsulated guests in aqueous media. The guests that bind most strongly to the polyanionic $[Ga_4L_6]^{12-}$ host have a single positive charge (reflecting the strong role played by aqueous solvation in determining the host–guest binding energy), but neutral guests are also bound, albeit more weakly, inside the host cavity.

We have determined that protonated bases are stabilized by encapsulation in the host. This property was put to work in the hydrolysis of compounds such as orthoformates and acetals, which require passage through transient protonated intermediates in order to undergo conversion in water to the corresponding carbonyl compounds. Dramatic rate accelerations (up to several thousand fold), relative to the background rate in aqueous solution, have been measured for substrates of optimal size and hydrophobicity. By carrying out careful studies of the mechanism of catalysis in the assembly, we identified enzyme-like Michaelis–Menten kinetic behavior for the catalyzed reactions. This has led to the conclusion that the potential energy surface (i.e, the mechanism) of the hydrolysis changes upon encapsulation. Although the reactions described in this Account have been carried out using the racemic host molecule, the assembly has recently been enantiomerically resolved, indicating that enantioselective protonation and catalysis is a future promising area of study.

This work was supported by the Director, Office of Science, Office of Basic Energy Sciences, and the Division of Chemical Sciences, Geosciences, and Biosciences of the U.S. Department of Energy at LBNL under Contract No. DE-AC02-05CH11231 and a NSF predoctoral fellowship to M.D.P.

BIOGRAPHICAL INFORMATION

Michael Pluth received his B.S. in chemistry and mathematics from the University of Oregon in 2004 working with David Tyler and his Ph.D. from the University of California, Berkeley, in 2008 under the joint direction of Kenneth Raymond and Robert Bergman. He is currently an NIH postdoctoral fellow with Stephen Lippard at the Massachusetts Institute of Technology.

Robert Bergman received his B.A. from Carleton College in 1963 and his Ph.D. from the University of Wisconsin in 1966 under the direction of Jerome Berson, followed by postdoctoral work with Ronald Breslow at Columbia University. He joined the faculty of the California Institute of Technology in 1967 and ten years later joined the faculty of the University of California, Berkeley. He has a long-standing interest in mechanistic chemistry and chemical reactivity that has recently expanded to the study of reactions in synthetic hosts in collaboration with Kenneth Raymond.

Kenneth Raymond received his B.A. from Reed College in 1964 and his Ph.D. from Northwestern University in 1968 under the joint direction of Fred Basolo and James Ibers. He joined the faculty of the University of California, Berkeley, in 1967. He has a long-standing interest in coordination chemistry, both synthetic and biological. More recently, his interest in supramolecular chemistry has expanded to the field of catalysis in collaboration with Robert Bergman.

FOOTNOTES

*To whom correspondence should be addressed. Fax: (+1) 510-642-7714 (Bergman); (+1) 510-486-5283 (Raymond). E-mail addresses: rbergman@berkeley.edu; raymond@socrates.berkeley.edu.

REFERENCES

1 Leininger, S.; Olenyuk, B.; Stang, P. J. Self-assembly of discrete cyclic nanostructures mediated by transition metals. *Chem. Rev.* **2000**, *100*, 853–907.

2 Vriezema, D. M.; Aragones, M. C.; Elemans, J.; Cornelissen, J.; Rowan, A. E.; Nolte, R. J. M. Self-assembled nanoreactors. *Chem. Rev.* **2005**, *105*, 1445–1489.

3 Ariga, K.; Hill, J. P.; Lee, M. V.; Vinu, A.; Charvet, R.; Acharya, S. Challenges and breakthroughs in recent research on self-assembly. *Sci. Technol. Adv. Mater.* **2008**, *9*, 1–96.

4 Bjerre, J.; Rousseau, C.; Marinescu, L.; Bols, M. Artificial enzymes, "Chemzymes": Current state and perspectives. *Appl. Microbiol. Biotechnol.* **2008**, *81*, 1–11.

5 Das, S.; Brudvig, G. W.; Crabtree, R. H. Molecular recognition in homogeneous transition metal catalysis: A biomimetic strategy for high selectivity. *Chem. Commun.* **2008**, 413–424.

6 Kleij, A. W.; Reek, J. N. H. Ligand-template directed assembly: An efficient approach for the supramolecular encapsulation of transition-metal catalysts. *Chem.—Eur. J.* **2006**, *12*, 4219–4227.

7 Koblenz, T. S.; Wassenaar, J.; Reek, J. N. H. Reactivity within a confined self-assembled nanospace. *Chem. Soc. Rev.* **2008**, *37*, 247–262.

8 Oshovsky, G. V.; Reinhoudt, D. N.; Verboom, W. Supramolecular chemistry in water. *Angew. Chem., Int. Ed.* **2007**, *46*, 2366–2393.

9 Motherwell, W. B.; Bingham, M. J.; Six, Y. Recent progress in the design and synthesis of artificial enzymes. *Tetrahedron* **2001**, *57*, 4663–4686.

10 Marinescu, L. G.; Bols, M. Very high rate enhancement of benzyl alcohol oxidation by an artificial enzyme. *Angew. Chem., Int. Ed.* **2006**, *45*, 4590–4593.

11 Iwasawa, T.; Hooley, R. J.; Rebek, J. Stabilization of labile carbonyl addition intermediates by a synthetic receptor. *Science* **2007**, *317*, 493–496.

12 Yebeutchou, R. M.; Dalcanale, E. Highly selective monomethylation of primary amines through host–guest product sequestration. *J. Am. Chem. Soc.* **2009**, *131*, 2452–2453.

13 Chen, J.; Rebek, J. Selectivity in an encapsulated cycloaddition reaction. *Org. Lett.* **2002**, *4*, 327–329.

14 Yoshizawa, M.; Tamura, M.; Fujita, M. Diels-Alder in aqueous molecular hosts: Unusual regioselectivity and efficient catalysis. *Science* **2006**, *312*, 251–254.

15 Shenoy, S. R.; Crisostomo, F. R. P.; Iwasawa, T.; Rebek, J. Organocatalysis in a synthetic receptor with an inwardly directed carboxylic acid. *J. Am. Chem. Soc.* **2008**, *130*, 5658–5659.

16 Caulder, D. L.; Raymond, K. N. Supermolecules by design. *Acc. Chem. Res.* **1999**, *32*, 975–982.

17 Caulder, D. L.; Powers, R. E.; Parac, T. N.; Raymond, K. N. The self-assembly of a predesigned tetrahedral M_4L_6 supramolecular cluster. *Angew. Chem., Int. Ed.* **1998**, *37*, 1840–1843.

18 Davis, A. V.; Fiedler, D.; Ziegler, M.; Terpin, A.; Raymond, K. N. Resolution of chiral, tetrahedral M_4L_6 metal-ligand hosts. *J. Am. Chem. Soc.* **2007**, *129*, 15354–15363.

19 Davis, A. V.; Raymond, K. N. The big squeeze: Guest exchange in an M_4L_6 supramolecular host. *J. Am. Chem. Soc.* **2005**, *127*, 7912–7919.

20 Pluth, M. D.; Johnson, D. W.; Szigethy, G.; Davis, A. V.; Teat, S. J.; Oliver, A. G.; Bergman, R. G.; Raymond, K. N. Structural consequences of anionic host–cationic guest interactions in a supramolecular assembly. *Inorg. Chem.* **2009**, *48*, 111–120.

21 Fiedler, D.; Leung, D. H.; Bergman, R. G.; Raymond, K. N. Selective molecular recognition, C-H bond activation, and catalysis in nanoscale reaction vessels. *Acc. Chem. Res.* **2005**, *38*, 349–358.

22 Hastings, C. J.; Fiedler, D.; Bergman, R. G.; Raymond, K. N. Aza Cope rearrangement of propargyl enammonium cations catalyzed by a self-assembled "nanozyme". *J. Am. Chem. Soc.* **2008**, *130*, 10977–10983.

23 Leung, D. H.; Bergman, R. G.; Raymond, K. N. Highly selective supramolecular catalyzed allylic alcohol isomerization. *J. Am. Chem. Soc.* **2007**, *129*, 2746–2747.

24 Brumaghim, J. L.; Michels, M.; Pagliero, D.; Raymond, K. N. Encapsulation and stabilization of reactive aromatic diazonium ions and the tropylium ion within a supramolecular host. *Eur. J. Org. Chem.* **2004**, 5115–5118.

25 Brumaghim, J. L.; Michels, M.; Raymond, K. N. Hydrophobic chemistry in aqueous solution: Stabilization and stereoselective encapsulation of phosphonium guests in a supramolecular host. *Eur. J. Org. Chem.* **2004**, 4552–4559.

26 Dong, V. M.; Fiedler, D.; Carl, B.; Bergman, R. G.; Raymond, K. N. Molecular recognition and stabilization of iminium ions in water. *J. Am. Chem. Soc.* **2006**, *128*, 14464–14465.

27 Pluth, M. D.; Bergman, R. G.; Raymond, K. N. Making amines strong bases: Thermodynamic stabilization of protonated guests in a highly-charged supramolecular host. *J. Am. Chem. Soc.* **2007**, *129*, 11459–11467.

28 Pluth, M. D.; Bergman, R. G.; Raymond, K. N. Encapsulation of protonated diamines in a water-soluble, chiral, supramolecular assembly allows for measurement of hydrogen-bond breaking followed by nitrogen inversion/rotation. *J. Am. Chem. Soc.* **2008**, *130*, 6362–6366.

29 Perrin, C. L.; Dwyer, T. J. Application of two-dimensional NMR to kinetics of chemical-exchange. *Chem. Rev.* **1990**, *90*, 935–967.

30 Pluth, M. D.; Fiedler, D.; Mugridge, J. S.; Bergman, R. G.; Raymond, K. N. Encapsulation and characterization of proton-bound amine homodimers in a water-soluble, self-assembled supramolecular host *Proc. Natl. Acad. Sci. U.S.A.* **2009**, *106*, 10438−10443.

31 Henao, J. D.; Suh, Y.-W.; Lee, J.-K.; Kung, M. C.; Kung, H. H. Striking confinement effect: $AuCl_4^-$ binding to amines in a nanocage cavity. *J. Am. Chem. Soc.* **2008**, *130*, 16142–16143.

32 Mohanty, J.; Bhasikuttan, A. C.; Nau, W. M.; Pal, H. Host−guest complexation of neutral red with macrocyclic host molecules: Contrasting pK_a shifts and binding affinities for cucurbit[7]uril and β-cyclodextrin. *J. Phys. Chem. B* **2006**, *110*, 5132–5138.

33 Praetorius, A.; Bailey, D. M.; Schwarzlose, T.; Nau, W. M. Design of a fluorescent dye for indicator displacement from cucurbiturils: A macrocycle-responsive fluorescent switch operating through a pK_a shift. *Org. Lett.* **2008**, *10*, 4089–4092.

34 Saleh, N.; Koner, A. L.; Nau, W. M. Activation and stabilization of drugs by supramolecular pK(a) shifts: Drug-delivery applications tailored for cucurbiturils. *Angew. Chem., Int. Ed.* **2008**, *47*, 5398–5401.

35 Shaikh, M.; Mohanty, J.; Singh, P. K.; Nau, W. M.; Pal, H. Complexation of acridine orange by cucurbit[7]uril and beta-cyclodextrin: Photophysical effects and pK(a) shifts. *Photochem. Photobiol. Sci.* **2008**, *7*, 408–414.

36 Biros, S. M.; Bergman, R. G.; Raymond, K. N. The hydrophobic effect drives the recognition of hydrocarbons by an anionic metal−ligand cluster. *J. Am. Chem. Soc.* **2007**, *129*, 12094–12095.

37 Hastings, C. J.; Pluth, M. D.; Biros, S. M.; Bergman, R. G.; Raymond, K. N. Simultaneously bound guests and chiral recognition: A chiral self-assembled supramolecular host encapsulates hydrophobic guests. *Tetrahedron* **2008**, *64*, 8362–8367.

38 Pluth, M. D.; Bergman, R. G.; Raymond, K. N. Acceleration of amide bond rotation by encapsulation in the hydrophobic interior of a water-soluble supramolecular assembly. *J. Org. Chem.* **2008**, *73*, 7132–7136.

39 Bell, R. P. *The Proton in Chemistry*, 2nd ed.; Cornell University Press: Ithica, NY, 1973.

40 Cordes, E. H.; Bull, H. G. Mechanism and catalysis for hydrolysis of acetals, ketals, and ortho esters. *Chem. Rev.* **1974**, *74*, 581–603.

41 Pluth, M. D.; Bergman, R. G.; Raymond, K. N. Acid catalysis in basic solution: A supramolecular host promotes orthoformate hydrolysis. *Science* **2007**, *316*, 85–88.

42 Pluth, M. D.; Bergman, R. G.; Raymond, K. N. Supramolecular catalysis of orthoformate hydrolysis in basic solution: An enzyme-like mechanism. *J. Am. Chem. Soc.* **2008**, *130*, 11423–11429.

43 Eadie, G. S. The inhibition of cholinesterase by physostigmine and prostigmine. *J. Biol. Chem.* **1942**, *146*, 85–93.

44 Hofstee, B. J. H. On the evaluation of the constants V_m and K_M in enzyme reactions. *Science* **1952**, *116*, 329–331.

45 Pluth, M. D.; Bergman, R. G.; Raymond, K. N. Catalytic deprotection of acetals in basic solution with a self-assembled supramolecular "nanozyme". *Angew. Chem., Int. Ed.* **2007**, *46*, 8587–8589.

46 Pluth, M. D.; Bergman, R. G.; Raymond, K. N. The acid hydrolysis mechanism of acetals catalyzed by a supramolecular assembly in basic solution. *J. Org. Chem.* **2009**, *74*, 58–63.

47 Krishnaveni, N. S.; Surendra, K.; Reddy, M. A.; Nageswar, Y. V. D.; Rao, K. R. Highly efficient deprotection of aromatic acetals under neutral conditions using β-cyclodextrin in water. *J. Org. Chem.* **2003**, *68*, 2018–2019.

48 Marko, I. E.; Ates, A.; Gautier, A.; Leroy, B.; Plancher, J. M.; Quesnel, Y.; Vanherck, J. C. Cerium(IV)-catalyzed deprotection of acetals and ketals under mildly basic conditions. *Angew. Chem., Int. Ed.* **1999**, *38*, 3207–3209.